International Journal of General Medicine

Dovepress
Taylor & Francis Group

Open Access Full Text Article

ORIGINAL RESEARCH

Compound Tinglizi Decoction-Containing Serum Is Associated with Inhibition of PANoptosis in Cardiomyocytes via SIRT3-Related Chaperone-Mediated Autophagy of AIM2

Ren Huang[1,*], Junyu Tang[2,*], Wenjuan Huang[1], Yan Shang[1], Wenli Liu[1], Huajun Long[1], Rongwen Wan[1]

[1]Department of Intensive Care Medicine, The Affiliated Hospital of Hunan Academy of Traditional Chinese Medicine, Changsha, Hunan, People's Republic of China; [2]Department of Geriatric Medicine, The Affiliated Hospital of Hunan Academy of Traditional Chinese Medicine, Changsha, Hunan, People's Republic of China

*These authors contributed equally to this work

Correspondence: Rongwen Wan, Department of Intensive Care Medicine, The Affiliated Hospital of Hunan Academy of Traditional Chinese Medicine, 58 Lushan Road, Yuelu District, Changsha, Hunan, 410006, People's Republic of China, Email wanrongwen007@163.com

Background: Septic cardiomyopathy (SCM) is a life-threatening complication of sepsis with no specific therapeutic options. Recent evidence suggests that PANoptosis, a programmed cell death pathway, contributes to myocardial injury in sepsis. Compound Tinglizi Decoction (CTLZC), a traditional Chinese herbal formula, has shown potential cardioprotective effects, yet the underlying biochemical mechanisms remain unclear.

Methods: A rat model of SCM was established to investigate the effect of CTLZC-containing serum on myocardial injury. Primary cardiomyocytes were treated with CTLZC-containing serum, and SIRT3 expression was modulated via overexpression and knockdown plasmids. Cell viability, PANoptosis markers, and chaperone-mediated autophagy (CMA) proteins were assessed through CCK-8, TUNEL staining, RT-qPCR, Western blotting, ELISA, and Co-IP assays.

Results: CTLZC-containing serum enhanced cardiomyocyte viability and significantly upregulated SIRT3 expression. It inhibited the expression of PANoptosis-related molecules (AIM2, ZBP1, RIPK1, RIPK3, FADD, and caspase-8) and promoted the expression of CMA-related proteins HSC70 and LAMP2A. SIRT3 knockdown reversed these effects and increased the release of biochemical markers of myocardial injury (LDH, CK-MB) and inflammatory cytokines (TNF-α, IL-1β, IL-18). Co-IP confirmed that AIM2 interacts with HSC70, indicating lysosomal degradation via CMA.

Conclusion: CTLZC-containing serum attenuates inflammatory and cell death responses in septic cardiomyopathy, likely through a SIRT3-associated modulation of chaperone-mediated autophagy and PANoptosis. These findings highlight the biochemical regulatory role of SIRT3 in mediating autophagic and inflammatory pathways during SCM, offering new insights into potential therapeutic targets.

Keywords: compound tinglizi decoction, cardiomyocytes, SIRT3, chaperone-mediated autophagy, PANoptosis

Introduction

Sepsis is a syndrome of systemic inflammatory response caused by invasion of pathogenic microorganisms and dysregulation of the body's response to infection. This systemic disease leads to multiple organ dysfunction and failure, with particular damage to the heart.[1,2] Septic cardiomyopathy (SCM) is one of the most prevalent complications of sepsis. Sepsis-induced myocardial injury and cardiac dysfunction further exacerbate tissue microcirculatory hypoperfusion, thereby initiating a vicious cycle that is closely associated with high morbidity and mortality from sepsis.[3,4] Epidemiological data indicate that the incidence of SCM is 18–40%, and that it is also an important factor affecting the

Received: 14 May 2025
Accepted: 18 October 2025
Published: 14 November 2025

prognosis of sepsis, with a case fatality rate of 70–90%. This imposes a significant burden on the patient's family and society.[5]

Compound Tinglizi Decoction (CTLZC), a traditional Chinese herbal formula composed of *Draba nemorosa* L., *Sinapis alba* L., *Solanum nigrum* L., *Trichosanthes kirilowii* Maxim., *Scleromitrion diffusum* (Willd)., and other well-known Chinese medicinal herbs, has been reported in limited studies to exert therapeutic effects, such as improving chronic obstructive pulmonary arterial hypertension.[6] However, direct evidence for its efficacy in septic cardiomyopathy remains scarce. Importantly, several of its herbal components or active ingredients—for example, triterpenoids from *Scleromitrion diffusum* (Willd)., and *Solanum nigrum* L.—have been shown to regulate oxidative stress, inflammation, and mitochondrial function.[7,8] Some of these compounds are capable of upregulating SIRT3 expression, thereby providing a pharmacological rationale that CTLZC-containing serum might confer cardioprotective effects through SIRT3-related mechanisms.

PANoptosis was first proposed by Kanneganti's team in Cell in 2021, where they introduced the new concept of PANoptosis, which encompasses the simultaneous occurrence of apoptosis, cellular pyroptosis and cell necrosis in inflammatory cell death.[9,10] Several studies have confirmed that PANoptosis is well validated in sepsis and that PANoptosis is a novel pathogenesis of sepsis, and that SARS-CoV, MERS-CoV and MHV can lead to cellular PANoptosis that promotes sepsis-induced acute lung injury.[9] However, its mediation of organ damage, including myocardial damage, remains unclear. AIM2 is a classical receptor protein that normally forms inflammatory vesicles with ACS and CASP1, recognizes pathogenic microbial invaders and binds to cytoplasmic double-stranded DNA, driving host responses and triggering inflammatory responses.[11] Given the pivotal role of the PANoptosome in the pathogenesis of PANoptosis, the timely inhibition of the functional role of the AIM2 receptor may represent a promising approach to the prevention and treatment of SCM.

Abnormal cardiomyocyte autophagy represents a key pathogenic mechanism in septic myocardial injury. Molecular chaperone-mediated autophagy (CMA), a process that selectively delivers proteins to the lysosome for degradation, plays an important role in the pathogenesis of sepsis. This process is responsible for the selective degradation of specific damaged or nonessential proteins.[12,13] It has been demonstrated that specific proteins with KFERQ-like motifs are recognized by HSC70 (HSPA8) and bind to LAMP2A to be transferred to the lysosome for degradation.[14] Sirtuin-3 (SIRT3), a NAD+-dependent histone deacetylase, is one of the key proteins newly identified to be able to attenuate sepsis-associated organ damage.[15–17] Since SIRT3 overexpression facilitates CMA activity by promoting the LAMP2A-Hsc70 complex,[18] and CTLZC active compounds have been shown to upregulate SIRT3, it is rational to hypothesize that CTLZC-containing serum may attenuate PANoptosis in cardiomyocytes via a SIRT3-CMA-AIM2 pathway.[19–23] However, direct evidence supporting this link remains limited, which constitutes the key research gap addressed in this study.

Materials and Methods

Reagents

Fetal bovine serum (FSD500) (Excell Bio, Beijing, China). Penicillin-streptomycin solution (100X) (C0222) (Beyotime, Shanghai, China). DMEM/F12 (11320033) (Gibco, Shanghai, China). Trypsin (R001100) (Gibco, Shanghai, China). Cell Freezing Solution (C0210B-50mL), PBS Buffer (C0221A) (Beyotime, Shanghai, China). Cell/Tissue Total RNA Isolation Kit V2 (RC112), HiScript lll 1st Strand cDNA Synthesis Kit (R312), Taq Pro Universal SYBR qPCR Master Mix (Q712) (Vazyme, Nanjing, China). Primers (Sangon, Shanghai, China). OE-SIRT3 and KD-SIRT3 and their NC plasmids were purchased from Suzhou Gemma Genetics Co. Ltd. and LipofectamineTM 3000 (L3000015) (Thermo Fisher, Waltham, MA, USA). APS (ST005), RIPA (P0013B), PMSF (ST506), TEMED (ST728) (Beyotime, Shanghai, China). 30% Acr/Bic (BL513A), Tris-Base (BS083), TBS buffer powder (BL602A), BSA protein standard (BL673A), Tween-20 (BS100) (Biosharp, Fuzhou, China). SDS (3250), Glycine (1275), Skimmed Milk (1172) (BioFroxx, Beijing, China). BCA Protein Content Determination Kit (WB6501), 5xSDS-PAGE Sampling Buffer (WB2001), ECL luminescent solution AB solution (P2100) (NCM Biotech, Shanghai, China). Prestained Protein Marker II (10–200 kDa) (G2058-250UL, Servicebio, Beijing, China). SirT3 (D22A3) Rabbit mAb #5490 (Cell Signaling Technology, Danvers, MA, USA). AIM2 Polyclonal antibody 20590-1-AP (Proteintech, Rosemont, IL, USA). Recombinant Anti-IGF2BP1 /IMP1 antibody [EPR26408-18] (ab290736) (Abcam, Cambridge, UK). RIPK1- specific polyclonal antibody 17519-1-AP (Proteintech, Rosemont, IL, USA). Anti-FADD antibody (ab216506) (Abcam, Cambridge, UK). RIP3 (D8J3L) Rabbit mAb #15828 (Cell Signaling Technology, Danvers, MA, USA). Recombinant Anti-Hsc70 antibody [EP1531Y] (ab51052) (Abcam, Cambridge, UK). Anti-Caspase-8 antibody (ab25901) (Abcam, Cambridge, UK). Recombinant Anti-LAMP2A antibody [EPR4207(2)] - Lysosome Marker (ab125068) (Abcam, Cambridge, UK). Western Antibody GAPDH-Loading Control (bsm-33033M) (Bioss, Wuhan, China). Goat Anti-Rabbit IgG H&L/HRP (bs-0295G-HRP) (Bioss, Wuhan, China). Goat Anti-Mouse IgG H&L/HRP (bs-0296G-HRP) (Bioss, Wuhan, China). Rat TNF-α ELISA KIT (SEKR-0009) (Solarbio, Beijing, China). Rat IL-1β ELISA KIT (SEKR-0002) (Solarbio, Beijing, China). Rat IL-18 Elisa Kit (SEKR-0054) (Solarbio, Beijing, China). Rat Lactate Dehydrogenase (LDH) ELISA Detection Kit (ml003416) (mlbio, Shanghai, China). Rat Creatine Kinase MB Isoenzyme (CKMB) ELISA Kit (JL12296-96T) (jonln, Shanghai, China). CCK8 Cell Proliferation Detection Kit (BA00208) (Bioss, Wuhan, China). Immunoprecipitation Kit (Protein A +G Magnetic Bead Assay) (P2179M), One Step TUNEL Detection Kit (Green Fluorescence) (C1086) (Beyotime, Shanghai, China).

Experimental Apparatus

Real-time fluorescence quantitative PCR instrument CFX96 Touch 1855195, Western blotting system (model: Criterion™ electrophoresis tank, Trans-blot® transfer tank) (Bio-Rad, Hercules, CA, USA). EVOS M5000 fluorescence microscope (Themo Fisher, Waltham, MA, USA). Optical microscope (Shanghai Optical Instrument No.1 Factory, Shanghai, China). JP-K6000 chemiluminescence analyzer (Shanghai Jiapeng, Shanghai, China). Ultra-low temperature refrigerator (Haier, Qingdao, China). RT-6000 Enzyme Analyser (Rayto, USA).

Constructing a Rat Model of Septic Cardiomyopathy

Male Sprague-Dawley (SD) rats (7–9 weeks old, SPF grade) were anesthetized by intraperitoneal injection of 0.3% sodium pentobarbital (10 mL/kg) and fixed, and the skin was prepared and disinfected routinely. A 1 cm incision was made along the ventral white line, and the cecum was extracted on the lower right side with toothless forceps and ligated at the cecum halfway with a sterile nylon suture. A puncture was then made at the bottom of the cecum with a 22G sterile syringe needle. The layers of tissue were closed sequentially with 2–3 stitches using moist 4–0 sutures. Following the procedure, the rats were provided with a diet and water supply. The cecal ligation and puncture (CLP) procedure used in this study has been widely recognized as a classical and reliable method for establishing a sepsis model.[21] The success of the model was confirmed based on typical clinical manifestations, including reduced activity, piloerection, and decreased food intake, together with a survival rate of approximately 60% within 48 h, which is consistent with previous reports.[22] Since our focus was to explore the mechanistic effect of CTLZC-containing serum rather than surgical trauma itself, a sham-operated group was not included.

Preparation of Drug-Containing Serum

A total of five rats were administered CTLZC (10.26 g/kg, which was selected based on previously reported effective doses in pharmacological studies and represents an intermediate value within the commonly used rang[6]) via oral gavage, while the control group received an equal volume of saline via oral gavage once daily. The CTLZC formula used in this study consists of *Draba nemorosa* L., *Sinapis alba* L., *Solanum nigrum* L., *Trichosanthes kirilowii* Maxim., *Scleromitrion diffusum* (Willd)., and other traditional Chinese medicinal herbs, which have been documented to exert regulatory effects on oxidative stress, inflammation, and mitochondrial function. The drug was administered continuously for 14 days. The blood was collected from the abdominal aorta following the administration of 3% pentobarbital sodium via intraperitoneal injection into the rats. The blood was then centrifuged at 3000 rpm for 30 min. The drug-containing serum is subjected to a 30-minute inactivation at 56°C, after which it is sterilized with a sterilized filter membrane and stored at −20°C. When required, the serum is to be diluted with F12K medium to the requisite concentration.

Primary Rat Cardiomyocyte Extraction and Culture

Following the construction of a rat model of septic cardiomyopathy over a period of 36 h, the rats were anaesthetized by the intraperitoneal injection of 0.3% sodium pentobarbital (10 mL/kg). The thoracic cavity was then opened for the rapid dissection of the heart, which was subsequently washed with PBS containing 20 mmol/L BDM. The hearts were immersed in 500 µL of isolation medium in a 24-well plate and cut into small pieces of approximately 1 mm^3 with curved scissors. The heart tissue was collected in a 15 mL tube containing 10 mL of cold isolation medium and gently agitated at 4°C overnight. On the second day, the majority of the supernatant was removed and 5mL of digestion medium was added. The heart tissue fragments were then digested at 37°C with gentle agitation for 30min, after which they were centrifuged at 300 r/min for 5 min. Following the aspiration of the supernatant, the cell precipitate was resuspended and incubated in spreading medium for a period of 3 h. During this time, fibroblasts and endothelial cells preferentially adhered to the culture dish and were removed by differential adhesion, as described in previous reports.[23] The approximate cardiomyocytes in the supernatant were collected and inoculated into DMEM/F12 medium containing 10% fetal bovine serum and placed in a 37°C, 5% CO_2 incubator for culture. The control group comprised extracted rat cardiomyocytes, while the low-, medium-, and high-dose CTLZC-containing serum groups (L-CTLZC, M-CTLZC, and H-CTLZC) were treated with 10%, 15%, and 20% CTLZC-containing serum, respectively. The pcDNA3.1-SIRT3 plasmid (SIRT3 overexpression, OE-SIRT3) or sh-SIRT3 plasmid (SIRT3 knockdown, KD-SIRT3) was transfected into cells to construct the overexpression and knockdown groups, respectively. Cells were treated for 24 h following transfection, and experiments were conducted using cardiomyocytes within passages 2–3 to ensure stability and viability.

CCK8 Assay for Cell Activity

Primary cardiomyocytes from the rat model of septic cardiomyopathy were inoculated in 96-well plates at a density of 2000 cells per well and incubated for 6 h at 37°C with 5% CO_2. The cells in each group were incubated for 24 h. Two hours before the end of the incubation period, 10 µL of CCK8 solution was added to each well. At the conclusion of the incubation period, the optical density at 450 nm was quantified via enzyme labeling.

TUNEL Staining

The TUNEL assay solution was configured using 30 µL TdT enzyme, 270 µL fluorescent labelling solution and 300 µL TUNEL. The cardiomyocytes of each group were fixed using 4% paraformaldehyde for 30 min, after which they were washed using PBS. They were then incubated with 0.3% Triton X-100 containing 0.3% Triton X-100 for 5min at room temperature.

Detection of Cellular LDH, CD-MK, TNF-α, IL-1β, and IL-18 Expression by ELISA

The supernatant of each group of cardiomyocytes was obtained, and the standard was diluted according to the instructions of the ELISA kit. The sample was added 50µL and incubated at 37°C for 30min. After washing, the enzyme-labeled reagent was added and the absorbance of each hole was measured at 450 nm.

Western Blot Detection of Protein Expression

Proteins were extracted using RIPA lysate and quantified using the BCA method. They were then separated by 10–12% SDS-PAGE gel electrophoresis (depending on the molecular weight of the target protein) and transferred to a PVDF membrane. Following a 2 h incubation at room temperature with 5% skimmed milk, the membrane was treated with appropriate primary antibodies overnight at 4°C. Secondary antibodies were then added, and the membranes were developed using a chemiluminescence imaging system. The dilution of primary and secondary antibodies is shown in Table 1. The grey scale analysis was conducted using the ImageJ software.

Real-Time PCR Analysis

The total cellular RNA was extracted using the TRIzol reagent. Purification of the RNA was achieved through a series of steps, including chloroform phase separation, isopropanol precipitation, and 75% ethanol washing. The cDNA was

Table 1 Antibody Were Diluted as Follows

Antibodies	Dilution (Application)
SIRT3	1:1000 (WB)
AIM2	1:1000 (WB)
ZBP1	1.0μg/mL (WB)
RIPK1	1:2000 (WB)
FADD	2μg/mL (WB)
RIPK3	1:1000 (WB)
Caspase-8	1μg/mL (WB)
HSC70	1:2000 (WB)
LAMP2A	1:2000 (WB)
GAPDH	1:10000 (WB)
Goat Anti-Rabbit IgG H&L(HRP)	1:20000 (WB)
Goat Anti-Mouse IgG H&L(HRP)	1:20000 (WB)

Table 2 Primers Used for RT-qPCR

Primers	Sequence (5′→3′)
AIM2	Forward: TCACCAGTTCCTCAGTTGTG
AIM2	Reverse: GGCTTTGCAGCCTTAATAACC
GAPDH	Forward: TGATGCTGGTGCTGAGTATGT
GAPDH	Reverse: TGATGTCATCATACTTGGCAGG

obtained by preparing a reverse transcription system and reacting at 25°C for 5 min, 42°C for 30 min, and 85°C for 5 min. A real-time quantitative polymerase chain reaction (PCR) reaction system was prepared and the reaction was performed using the CFX96 Touch 1855195 Real-time Fluorescence Quantitative PCR Instrument. The following procedure was employed: pre-denaturation at 95°C for 30s, denaturation at 95°C for 10s. The annealing temperature was set at 60°C for 10s, the extension temperature at 95°C for 15s, and the cycle count was set at 40. The melting curve was set at 60°C for 60s and 95°C for 15s. The experimental results were calculated using the $2^{-\Delta\Delta Ct}$ method. The primer sequences were listed in Table 2.

Co-IP

Cardiomyocytes were collected, 500 μL of cell lysis buffer was added per sample, and the supernatant was centrifuged at 12,000× g for 10 min at 4°C. For each reaction, 2 μg of the indicated antibody (chosen based on previous reports for sufficient binding efficiency) and 5 μL protein A/G beads were added to the cell lysate and incubated slowly at 4°C overnight. After the immunoprecipitation reaction, the protein A/G beads were centrifuged at 3000 rpm for 5 min at 4°C. The supernatant was removed and the Protein A/G beads were washed three times with 1 mL lysis buffer, each wash lasting 5 min at 4°C with gentle mixing. 20 μL of 2× SDS spiking buffer was added and boiled for 5min to elute the bound protein complexes. The eluted proteins were then subjected to SDS-PAGE followed by Western blotting. Primary antibodies used after Co-IP included anti-Hsc70 and anti-AIM2 to verify the interaction between these proteins. Protein samples were separated by SDS-PAGE gel and detected by membrane transfer, capture, primary antibody incubation, secondary antibody incubation and development. And the results of immunoprecipitation were analyzed.

Statistical Analysis

The data were analyzed and plotted using Graphpad Prism 9 (version 9.4.0). All data are expressed as mean ± SD. Statistical differences between groups were tested using *T*-test or one-way ANOVA followed by Post Hoc Test (Least Significant Difference), with *P* values less than 0.05 considered significant.

Results

Validating the Occurrence of PANoptosis in Cardiomyocytes in a Rat Sepsis Model and Exploring the Mitigating Effect of CTLZC on Inflammatory Injury

To verify the role of CTLZC in the prevention of inflammatory injury in septic cardiomyopathy, a rat sepsis model was first constructed and cardiomyocytes extracted to investigate the occurrence of PANoptosis. Three concentrations of CTLZC were then administered to the myocardial injury cell model, with cell activity and death levels observed by CCK8 and TUNEL staining. As shown in Figure 1a and b, 10% and 15% CTLZC were found to promote cardiomyocytes proliferative activity and inhibit cell death. However, CTLZC at 20% was observed to have an attenuating effect on the fine proliferative activity. Subsequently, we employed Western blot analysis to assess the impact of 10% CTLZC intervention on protein expression levels. Our findings revealed a significant increase in SIRT3 expression ($P<0.01$). The expression level of PANoptosis receptor protein AIM2 was found to be significantly reduced ($P<0.001$), as were the expression levels of PANoptosis-related proteins ZBP1, RIPK1, FADD, RIPK3, and caspase-8 ($P<0.01$) (Figure 1c and d). The results demonstrated that PANoptosis occurred in cardiomyocytes in the rat sepsis model, and that CTLZC was able to inhibit the level of PANoptosis in septic cardiomyocytes.

AIM2 Has a Potential HSC70-Specific Binding Motif (KVDKQ) and SIRT3 Promotes Lysosomal Degradation of AIM2 Molecular Chaperones Mediating Autophagy

In the aforementioned experiments, a negative correlation was observed between AIM2 protein levels and SIRT3. The AIM2 protein sequence was analyzed using the UniProtKB database (https://www.uniprot.org/uniprotkb/) to gain further insight into the protein sequence. Interestingly, we identified a potential HSC70-specific binding motif (KVDKQ) that may activate the CMA degradation mechanism (Figure 2a). Plasmids for overexpression and knockdown of SIRT3 were constructed and transfected into cardiomyocytes. The expression levels of molecular chaperone-mediated autophagy-related proteins HSC70 and LAMP2A were detected by Western Blot, and the results demonstrated that overexpression of SIRT3 promoted the expression of HSC70 and LAMP2A, while knockdown of SIRT3 inhibited the expression of HSC70 and LAMP2A (Figure 2b) ($P<0.01$).

Furthermore, we examined AIM2 expression levels by RT-qPCR and Western blot. As illustrated in Figure 2c and d, overexpression of SIRT3 resulted in a reduction in AIM2 mRNA ($P<0.05$) and protein levels ($P<0.01$), whereas knockdown of SIRT3 led to an increase in AIM2 mRNA ($P<0.001$) and protein levels ($P<0.001$). We investigated the binding role of AIM2 to HCS70 by Co-IP. In addition, we performed in vitro binding assays to probe the binding role of AIM2 to HCS70 by Co-IP. As anticipated, the results showed that HSC70 could interact with AIM2 in vitro (Figure 2e). The results indicate that SIRT3 plays a role in the lysosomal degradation of AIM2 molecular chaperones, which is essential for autophagy.

CTLZC Ameliorates Cardiomyocytes PANoptosis Through SIRT3-Promoted AIM2 CMA Degradation Mechanism

The objective of this study was to investigate whether CTLZC may ameliorate PANoptosis in septic cardiomyocytes through SIRT3-related pathways. To this end, the effects of intervening with CTLZC and knocking down SIRT3 on cardiomyocytes PANoptosis were first observed by TUNEL staining. As illustrated in Figure 3a, TUNEL-positive dead cells were labelled with green fluorescence, and the number of green fluorescence-positive cells was significantly elevated in the SIRT3 knockdown combined with CTLZC intervention group in comparison to the CTLZC intervention group ($P<0.001$). Furthermore, the expression of myocardial injury markers LDH and CK-MB in cell supernatants was detected by ELISA. The results demonstrated that the expression levels of LDH and CK-MB were significantly reduced in the CTLZC group in comparison to the Control group ($P<0.001$) (Figure 3b). In comparison to the CTLZC group, the expression levels of LDH and CK-MB were found to be significantly elevated in the KD-SIRT3+CTLZC group ($P<0.001$).

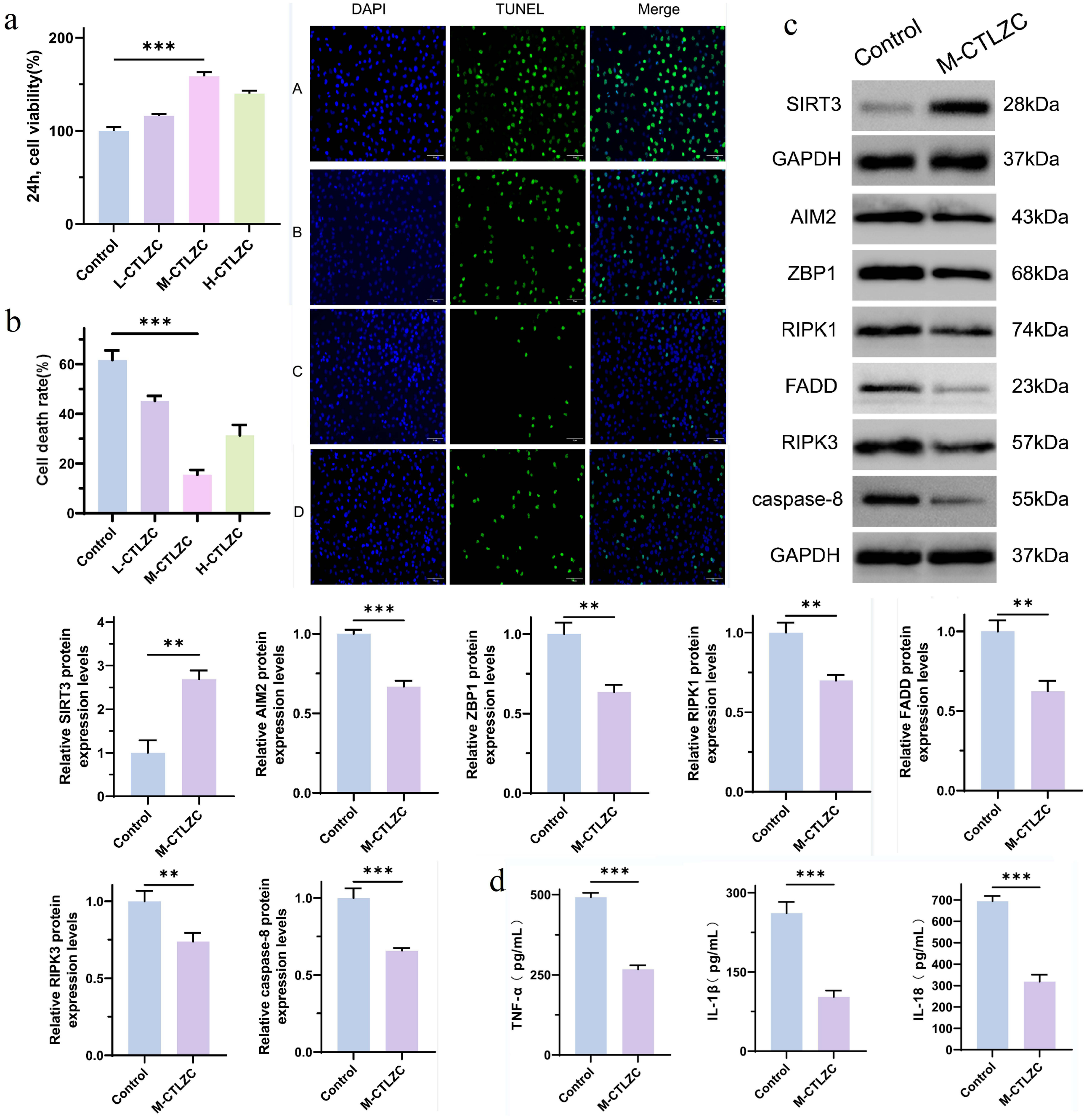

Figure 1 Detection of cell proliferation, apoptosis, protein expression and inflammatory factor levels. (**a**) CCK8 detects cell proliferation activity. (**b**) TUNEL staining to observes cell death [(A) Control group, (B) Low dose (10% serum, L-CTLZC), (C) Medium dose (15% serum, M-CTLZC), (D) High dose (20% serum, H-CTLZC)]. (**c**) Western Blot detects the expression of SIRT3, AIM2, ZBP1, RIPK1, FADD, RIPK3, caspase-8. (**d**) ELISA detects expression of TNF-α, IL-1β and IL-18. Data are presented as mean ± SD (n = 3 independent experiments). Statistical significance was determined by one-way ANOVA followed by LSD post-hoc test. $^{**}P < 0.01$, $^{***}P < 0.001$ vs Control.

Subsequently, we examined the expression levels of AIM2 and PANoptosis-related proteins by Western Blot. As shown in Figure 4a, CTLZC was able to down-regulate the protein expression levels of AIM2, ZBP1, RIPK1, FADD, RIPK3, caspase-8, HSC70, and LAMP2A ($P<0.01$). The expression levels of AIM2 and PANoptosis-related proteins were found to be significantly elevated in the KD-SIRT3+CTLZC group in comparison to those observed in the CTLZC group (Figure 4b) ($P<0.001$). We also detected the expression levels of inflammatory factors in the cell supernatant by ELISA, and CTLZC was able to significantly inhibit the secretion levels of TNF-α, IL-1β, and IL-18 compared to the Control group (Figure 4c) ($P<0.001$). When SIRT3 was knocked down, the reduced level of inflammatory factors by

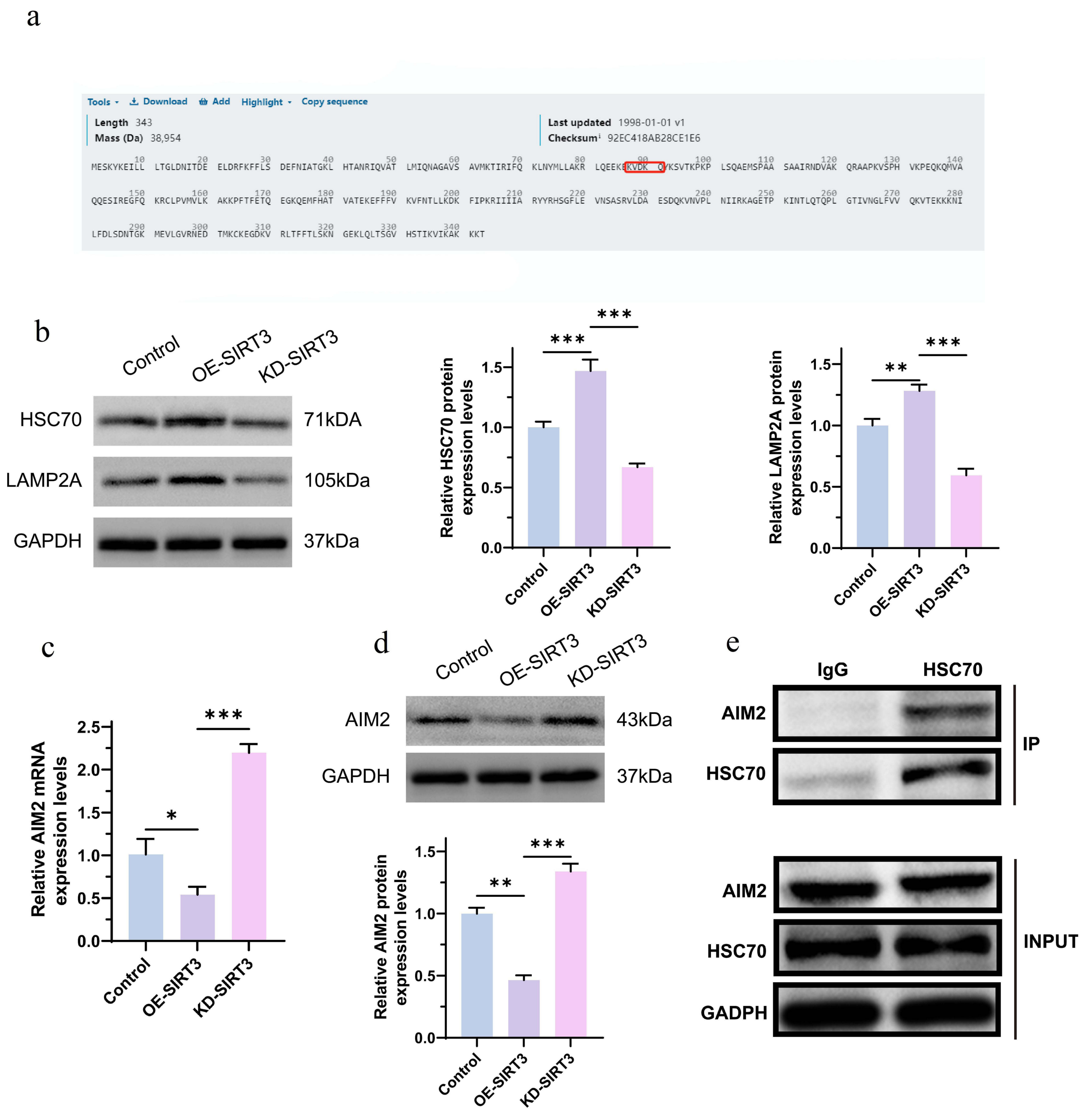

Length 343
Mass (Da) 38,954
Last updated 1998-01-01 v1
Checksum 92EC418AB28CE1E6

```
        10         20         30         40         50         60         70         80         90        100        110        120        130        140
MESKYKEILL LTGLDNITDE ELDRFKFFLS DEFNIATGKL HTANRIQVAT LMIQNAGAVS AVMKTIRIFQ KLNYMLLAKR LQEEKEKVDK QYKSVTKPKP LSQAEMSPAA SAAIRNDVAK QRAAPKVSPH VKPEQKQMVA

       150        160        170        180        190        200        210        220        230        240        250        260        270        280
QQESIREGFQ KRCLPVMVLK AKKPFTFETQ EGKQEMFHAT VATEKEFFFV KVFNTLLKDK FIPKRIIIIA RYYRHSGFLE VNSASRVLDA ESDQKVNVPL NIIRKAGETP KINTLQTQPL GTIVNGLFVV QKVTEKKKNI

       290        300        310        320        330        340
LFDLSDNTGK MEVLGVRNED TMKCKEGDKV RLTFFTLSKN GEKLQLTSGV HSTIKVIKAK KKT
```

Figure 2 To detect the expression levels of CMA-related proteins, AIM2, and to verify the binding of AIM2 to HCS70. (**a**) Protein sequence of AIM2 showing the putative HSC70 binding motif (KVDKQ) highlighted in red. (**b**) Western Blot detects the expression of HSC70 and LAMP2A. (**c**) RT-qPCR detects the expression of AIM2. (**d**) Western blot detects the expression of AIM2. (**e**) The protein expression levels of AIM2 and HSC70 were detected by immunoprecipitation with HSC70 antibody in Co-IP buffer for in vitro pull-down assay combined with Western Blot. Data are presented as mean ± SD (n = 3 independent experiments). Statistical significance was determined by one-way ANOVA followed by LSD post-hoc test. *$P < 0.05$, **$P < 0.01$, ***$P < 0.001$ vs OE-SIRT3.

CTLZC was significantly inhibited. Taken together, these results suggest that CTLZC improves cardiomyocytes PANoptosis in a SIRT3-dependent manner and is associated with CMA-related degradation of AIM2.

Discussion

The process of PANoptosis is regulated by the pan-apoptotic vesicle complex (PANoptosome), which is regulated by a cascade of receptors and molecular signals upstream of the pan-apoptotic machinery. The assembly of the PANoptosome as well as the activation of PANoptosis is a self-protective response for the body to effectively defend

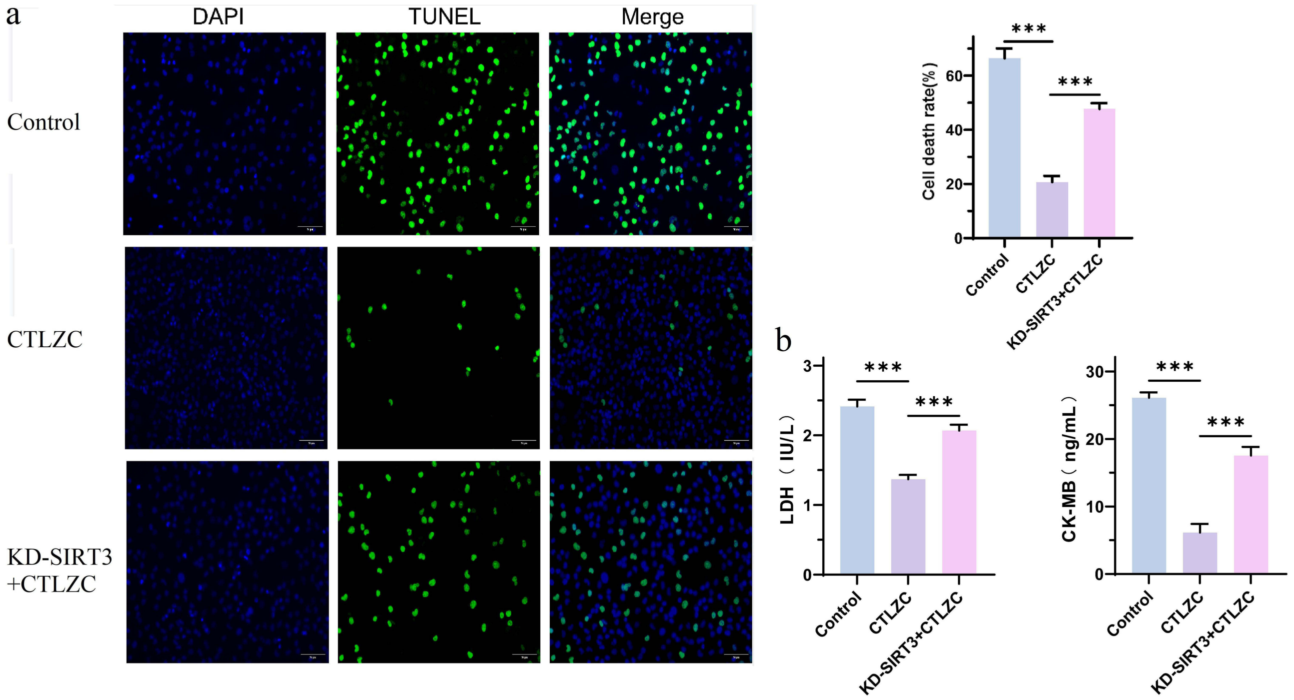

Figure 3 Detection of cell activity and analyses (**a**) TUNEL staining to observe cell death. (**b**) The content of LDH and CK-MB markers of myocardial injury detected by ELISA. Data are presented as mean ± SD (n = 3 independent experiments). Statistical significance was determined by one-way ANOVA followed by LSD post-hoc test. $^{***}P < 0.001$ vs CTLZC.

itself against foreign viral, bacterial, and fungal infections.[24] Lee et al[25] demonstrated that AIM2 regulates the downstream receptors pyrin and ZBP1, driving the formation of the pan-apoptotic complex and inducing the onset of cellular PANoptosis in HSV1- and Francisella-infected bone marrow-derived macrophage cells and animal models. It is notable that the activation of AIM2 inflammatory vesicles is involved in the progression of sepsis.[26] AIM2 knockdown has been shown to attenuate oxidative stress and inflammatory damage in myocardial tissue in diabetic cardiomyopathy.[27] In line with these reports, our data verified the presence of PANoptosis in cardiomyocytes from the sepsis model and identified SIRT3 as a requisite node for the protective effects of CTLZC-containing serum. Importantly, we describe this effect as SIRT3-dependent while being associated with, rather than conclusively mediated by, CMA-driven degradation of AIM2.

We summarize the key observations as follows: (i) CTLZC-containing serum improved cell viability and reduced inflammatory readouts in septic cardiomyocytes; (ii) genetic modulation of SIRT3 (overexpression/knockdown) respectively enhanced or attenuated these benefits, indicating SIRT3 dependence; and (iii) AIM2 interacted with HSC70 and changes in HSC70/LAMP2A accompanied SIRT3 manipulation, suggesting a potential CMA link. Given that Co-IP evidences protein–protein interaction but does not by itself establish lysosomal CMA flux or substrate degradation causality, we cautiously interpret the CMA involvement as a correlation that warrants further validation.

Scapularia japonica, Scutellaria baicalensis, Atractylodes macrocephala, and Licorice in CTLZC have been demonstrated to possess the ability to improve the inhibition of cardiomyocyte apoptosis and myocardial fibrosis, as well as to improve the indicators of myocardial injury.[28] It has been reported that baicalin, the active ingredient in Scutellaria baicalensis, may upregulate SIRT3 protein expression through inhibition of the proteasome and activation of PSMB5.[19] Poria cocos acid A, the active ingredient in Poria cocos, and atractylenolide, the active ingredient in Atractylodes macrocephala, may upregulate SIRT3 to exert biological effects.[20,29] Many studies have confirmed that glycyrrhizin, the active constituent of Licorice, is able to increase SIRT3 levels and decrease ROS, pro-inflammatory mediators and MMP expression. Additionally, glycyrrhetinic acid, the active constituent, has been shown to facilitate SIRT3 transcription and up-regulate SIRT3 levels by promoting the nuclear translocation of NRF2.[30,31] The present study demonstrated that CTLZC was capable of upregulating SIRT3 protein expression levels, enhancing cardiomyocyte activity, inhibiting cell death, and reducing markers of myocardial injury. These prior observations provide a pharmacological rationale for

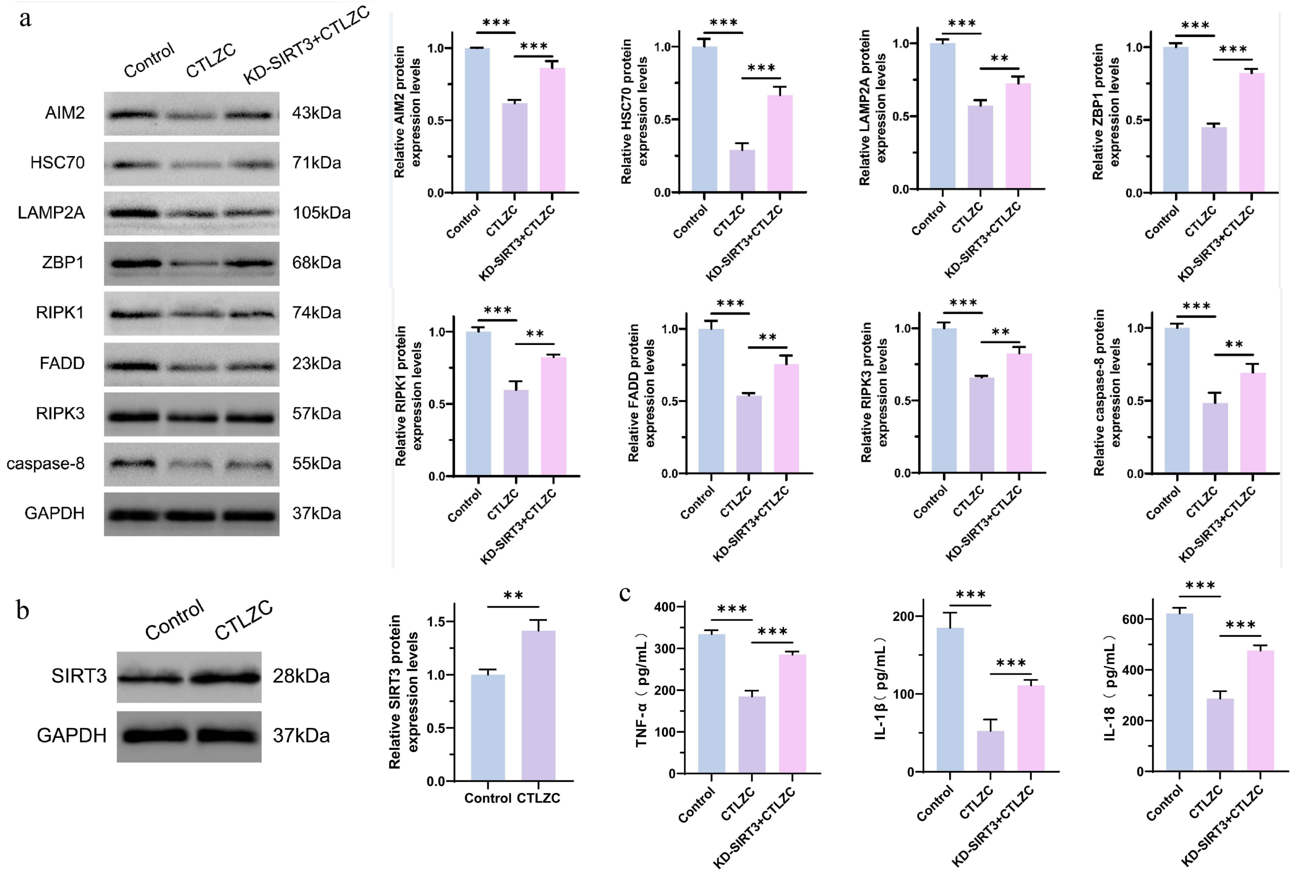

Figure 4 Detection of protein expression and inflammatory factor expression levels. (**a**) Western Blot detects the expression levels of AIM2, ZBP1, RIPK1, FADD, RIPK3, caspase-8, HSC70, and LAMP2A proteins. (**b**) Western Blot detects the expression of SIRT3. (**c**) ELISA detects expression of TNF-α, IL-1β, and IL-18. Data are presented as mean ± SD (n = 3 independent experiments). Statistical significance was determined by one-way ANOVA followed by LSD post-hoc test. $^{**}P < 0.01$, $^{***}P < 0.001$.

SIRT3 engagement by CTLZC-containing serum in our model, and strengthen the biological plausibility that upstream constituents could converge on SIRT3-regulated stress and mitochondrial pathways.

The activation of autophagy has been demonstrated to play a protective role in the regulation of excessive inflammatory factors in septic organisms.[32] Qiao et al[33] have identified a link between defects in CMA and the activation of NLRP3 inflammatory vesicles, which in turn has been shown to exacerbate inflammatory responses. In a study by Li et al[13] it was demonstrated that reduced protein expression of Lamp2A and Hsc70, markers of chaperone-mediated autophagy (CMA) activity in sepsis-associated encephalopathy (SAE), and the promotion of CMA activity ameliorated cognitive deficits and neuronal loss in SAE mice through the regulation of p-CREB, BDNF, BCL-2, and cleaved caspase-3. In the context of the CMA mechanism, the capacity of HSC70 to bind to motifs is primarily contingent upon the nature of the residues that comprise the motifs, rather than a specific and idiosyncratic amino acid sequence.[34,35] Zhao et al[35] demonstrated that TANK-binding kinase 1 (TBK1) possesses a canonical CMA motif (KFDKQ), and that USP19 facilitates lysosomal degradation of TBK1 via CMA. In vivo and in vitro experiments have corroborated that USP19 deletion results in elevated TBK1 and type I interferon activation, which are implicated in the regulation of the innate immune response process of the virus. In our study, SIRT3 overexpression coincided with higher HSC70/LAMP2A levels and reduced AIM2 abundance, while SIRT3 knockdown showed the opposite pattern, supporting a model in which SIRT3 activation is associated with enhanced CMA components and AIM2 turnover. Future studies using lysosomal inhibitors, CMA blockade, and degradation kinetics will be essential to demonstrate CMA-dependent AIM2 degradation and thereby move beyond correlation. To our knowledge, this is the first report to delineate that the anti-PANoptotic effects of CTLZC-containing serum in septic cardiomyocytes are SIRT3-dependent, and to propose a mechanistic link connecting SIRT3, CMA machinery, and AIM2 as a putative substrate hub. This SIRT3–CMA–AIM2 axis offers a coherent framework integrating mitochondrial stress responses with inflammatory cell-death checkpoints in sepsis, and suggests testable therapeutic entry points at SIRT3 activation and CMA facilitation.

However, this study still has certain limitations. First, we did not directly analyze the chemical constituents of CTLZC-containing serum, and future studies combining LC-MS/MS profiling with pharmacokinetic assessment are needed to identify specific compounds responsible for SIRT3 upregulation. Second, a sham-operated group was not included in the in vivo experiments; although our focus was on the mechanistic interrogation of CTLZC-containing serum in septic cardiomyocytes, future work should incorporate sham controls to strengthen the experimental design. Third, Figure 4b only displays the expression of SIRT3, and the KD-SIRT3+CTLZC group was not included in this panel because this combination was not tested under the Western blot setting; nevertheless, its effects on myocardial injury markers were evaluated in Figure 3 and showed consistent trends.

Conclusion

In conclusion, the results demonstrate that CTLZC significantly inhibits the onset of PANoptosis in a rat sepsis model of cardiomyocytes, upregulates the expression level of SIRT3, promotes the expression of HSC70 and LAMP2A proteins in CMA, and inhibits the expression of protein levels of AIM2, ZBP1, RIPK1, and FADD. Furthermore, it reduces the levels of myocardial injury markers and inflammatory factors in PANoptosis. However, it is important to note that this study has limitations. For instance, in vivo experiments have demonstrated that CTLZC exerts a protective effect against septic myocardial injury by modulating SIRT3-AIM2-PANoptosis. The objective of this study was to investigate the pathological mechanisms underlying septic myocardial injury and to identify potential targets for intervention.

Data Sharing Statement

The data presented in this study are available on request from the corresponding author.

Ethics Approval and Consent to Participate

This study was approved by the Animal Ethics Committee of The Affiliated Hospital of Hunan Academy of Traditional Chinese (Approval No. 23-HTC-A03). The care and use of laboratory animals complied with the National Institutes of Health Guide for the Care and Use of Laboratory Animals and the Guidelines for the Ethical Review of Laboratory Animal Welfare.

Acknowledgments

The authors express their appreciation to staff in The Affiliated Hospital of Hunan Academy of Traditional Chinese Medicine, for their technical assistance.

Author Contributions

All authors made a significant contribution to the work reported, whether that is in the conception, study design, execution, acquisition of data, analysis and interpretation, or in all these areas; took part in drafting, revising or critically reviewing the article; gave final approval of the version to be published; have agreed on the journal to which the article has been submitted; and agree to be accountable for all aspects of the work.

Funding

This study was not supported by any sponsor or funder.

Disclosure

The authors declare that they have no conflicts of interest in this work.

References

1. Ehrman RR, Sullivan AN, Favot MJ, et al. Pathophysiology, echocardiographic evaluation, biomarker findings, and prognostic implications of septic cardiomyopathy: a review of the literature. *Crit Care*. 2018;22(1):112. doi:10.1186/s13054-018-2043-8

2. Lim GB. Cardiac-resident macrophages protect against sepsis-induced cardiomyopathy. *Nat Rev Cardiol*. 2023;20(3):141. doi:10.1038/s41569-023-00837-7
3. Hollenberg SM, Singer M. Pathophysiology of sepsis-induced cardiomyopathy. *Nat Rev Cardiol*. 2021;18(6):424–434. doi:10.1038/s41569-020-00492-2
4. Wang R, Xu Y, Fang Y, et al. Pathogenetic mechanisms of septic cardiomyopathy. *J Cell Physiol*. 2022;237(1):49–58. doi:10.1002/jcp.30527
5. Ravikumar N, Sayed MA, Poonsuph CJ, et al. Septic cardiomyopathy: from basics to management choices. *Curr Prob Cardiol*. 2021;46(4):100767. doi:10.1016/j.cpcardiol.2020.100767
6. Wu X, Liu Y, Bai Z. Compound Tinglizi Decoction intervenes COPD-associated pulmonary hypertension through regulation of HMGB1-mediated pyroptosis and immune imbalance. *Zhongguo Zhong Yao Za Zhi*. 2023;48(11):3055–3065. doi:10.19540/j.cnki.cjcmm.20221014.702
7. Ho Y, Au T, Wu H, et al. Comparative study of scleromitrion diffusum and oldenlandia corymbosa: microscopy, TLC, HPLC, and antioxidant activity. *Microsc Res Techniq*. 2024;87(10):2371–2384. doi:10.1002/jemt.24611
8. Wang X, Sun Z, Wang X, et al. Solanum nigrum L. berries extract ameliorated the alcoholic liver injury by regulating gut microbiota, lipid metabolism, inflammation, and oxidative stress. *Food Res Int*. 2024;188:114489. doi:10.1016/j.foodres.2024.114489
9. Karki R, Sharma BR, Tuladhar S, et al. Synergism of TNF-alpha and IFN-gamma triggers inflammatory cell death, tissue damage, and mortality in SARS-CoV-2 infection and cytokine shock syndromes. *Cell*. 2021;184(1):149–168. doi:10.1016/j.cell.2020.11.025
10. Zhu P, Ke ZR, Chen JX, et al. Advances in mechanism and regulation of PANoptosis: prospects in disease treatment. *Front Immunol*. 2023;14:1120034. doi:10.3389/fimmu.2023.1120034
11. Onodi Z, Ruppert M, Kucsera D, et al. AIM2-driven inflammasome activation in heart failure. *Cardiovasc Res*. 2021;117(13):2639–2651. doi:10.1093/cvr/cvab202
12. Kaushik S, Cuervo AM. The coming of age of chaperone-mediated autophagy. *Nat Rev Mol Cell Bio*. 2018;19(6):365–381. doi:10.1038/s41580-018-0001-6
13. Li Y, Fan Z, Jia Q, et al. Chaperone-mediated autophagy (CMA) alleviates cognitive impairment by reducing neuronal death in sepsis-associated encephalopathy (SAE). *Exp Neurol*. 2023;365:114417. doi:10.1016/j.expneurol.2023.114417
14. Yang Q, Wang R, Zhu L. Chaperone-Mediated Autophagy. *Adv Exp Med Biol*. 2019;1206:435–452. doi:10.1007/978-981-15-0602-4_20
15. Wang J, Li W, Zhao F, et al. Sirt3 regulates NLRP3 and participates in the effects of plantainoside D on acute lung injury sepsis. *Aging*. 2023;15(14):6710–6720. doi:10.18632/aging.204628
16. Wu Z, Wang Y, Lu S, et al. SIRT3 alleviates sepsis-induced acute lung injury by inhibiting pyroptosis via regulating the deacetylation of FoxO3a. *Pulm Pharmacol Ther*. 2023;82:102244. doi:10.1016/j.pupt.2023.102244
17. Qin S, Ren YC, Liu JY, et al. ANXA1sp attenuates sepsis-induced myocardial injury by promoting mitochondrial biosynthesis and inhibiting oxidative stress and autophagy via SIRT3 upregulation. *Kaohsiung J Med Sci*. 2024;40(1):35–45. doi:10.1002/kjm2.12767
18. Zhang T, Liu J, Shen S, et al. SIRT3 promotes lipophagy and chaperon-mediated autophagy to protect hepatocytes against lipotoxicity. *Cell Death Differ*. 2020;27(1):329–344. doi:10.1038/s41418-019-0356-z
19. Cai Y, Jiang S, Huang C, et al. Baicalin inhibits pressure overload-induced cardiac hypertrophy by regulating the SIRT3-dependent signaling pathway. *Phytomedicine*. 2023;114:154747. doi:10.1016/j.phymed.2023.154747
20. Chen DQ, Chen L, Guo Y, et al. Poricoic acid A suppresses renal fibroblast activation and interstitial fibrosis in UUO rats via upregulating Sirt3 and promoting beta-catenin K49 deacetylation. *Acta Pharmacol Sin*. 2023;44(5):1038–1050. doi:10.1038/s41401-022-01026-x
21. Wu J, Tsou M, Chen T, et al. Therapeutic effects of melatonin on peritonitis-induced septic shock with multiple organ dysfunction syndrome in rats. *J Pineal Res*. 2008;45(1):106–116. doi:10.1111/j.1600-079X.2008.00567.x
22. Capcha JMC, Moreira RS, Rodrigues CE, et al. Using the cecal ligation and puncture model of sepsis to induce rats to multiple organ dysfunction. *Bio-Protocol*. 2021;11(7):e3979. doi:10.21769/BioProtoc.3979
23. Zimmer A, Wang ER, Choudhary G, et al. Protocol for simultaneous isolation of high-quality and high-quantity cardiomyocytes and non-myocyte cells from adult rat hearts. *Star Protoc*. 2024;5(3):103174. doi:10.1016/j.xpro.2024.103174
24. Samir P, Malireddi R, Kanneganti TD. The PANoptosome: a deadly protein complex driving pyroptosis, apoptosis, and necroptosis (PANoptosis). *Front Cell Infect Mi*. 2020;10:238. doi:10.3389/fcimb.2020.00238
25. Lee S, Karki R, Wang Y, et al. AIM2 forms a complex with pyrin and ZBP1 to drive PANoptosis and host defence. *Nature*. 2021;597(7876):415–419. doi:10.1038/s41586-021-03875-8
26. Xie M, Yu Y, Kang R, et al. PKM2-dependent glycolysis promotes NLRP3 and AIM2 inflammasome activation. *Nat Commun*. 2016;7:13280. doi:10.1038/ncomms13280
27. Li Q, Liu Y, Meng J, et al. Role of AIM2 gene knockdown mechanism in diabetic cardiomyopathy: an in vivo and ex vivo study. *Appl Biochem Biotech*. 2023;195(6):3533–3545. doi:10.1007/s12010-022-04306-8
28. Yang MQ, Chen C, Mao YF, et al. Application of network pharmacology and molecular docking approach to explore active compounds and potential pharmacological mechanisms of aconiti lateralis radix praeparata and lepidii semen descurainiae semen for treatment of heart failure. *Medicine*. 2022;101(33):e30102. doi:10.1097/MD.0000000000030102
29. Sun S, Shi J, Wang X, et al. Atractylon inhibits the tumorigenesis of glioblastoma through SIRT3 signaling. *Am J Cancer Res*. 2022;12(5):2310–2322.
30. Zhou M, Dai Y, Ma Y, et al. Protective effects of liquiritigenin against cisplatin-induced nephrotoxicity via NRF2/SIRT3-mediated improvement of mitochondrial function. *Molecules*. 2022;27(12). doi:10.3390/molecules27123823
31. Li Y, Xia C, Yao G, et al. Protective effects of liquiritin on UVB-induced skin damage in SD rats. *Int Immunopharmacol*. 2021;97:107614. doi:10.1016/j.intimp.2021.107614
32. Qi Z, Liu R, Ju H, et al. microRNA-130b-3p attenuates septic cardiomyopathy by regulating the AMPK/mTOR signaling pathways and directly targeting ACSL4 against ferroptosis. *Int J Biol Sci*. 2023;19(13):4223–4241. doi:10.7150/ijbs.82287
33. Qiao L, Ma J, Zhang Z, et al. Deficient chaperone-mediated autophagy promotes inflammation and atherosclerosis. *Circ Res*. 2021;129(12):1141–1157. doi:10.1161/CIRCRESAHA.121.318908
34. Song H, Huang W, Jia F, et al. Targeted degradation of signal transduction and activator of transcription 3 by chaperone-mediated autophagy targeting chimeric nanoplatform. *Acs Nano*. 2024;18(2):1599–1610. doi:10.1021/acsnano.3c09536
35. Zhao X, Di Q, Yu J, et al. USP19 (ubiquitin specific peptidase 19) promotes TBK1 (TANK-binding kinase 1) degradation via chaperone-mediated autophagy. *Autophagy.* 2022;18(4):891–908. doi:10.1080/15548627.2021.1963155